

## 1. Overview

We propose to combine multi-wavelength data to probe the gas and dust in galaxies in two nearby filaments to constrain the physical mechanisms that cause galaxies to evolve from blue, actively star-forming galaxies to red, passive galaxies. We will focus on where and how passage into a filamentary structure affects a galaxy's gas supply. Specifically, we will measure the spatial extent of the dust and star-forming disks relative to the stellar disk for  $\sim 200$  galaxies that reside in the large-scale filaments surrounding the Virgo cluster. We will combine this information with measurements of molecular gas and atomic hydrogen to create a complete census of the interstellar medium for a large sample of galaxies in this dynamic environment.

Virgo is one of the best studied clusters, period. We will our gas and dust properties of filament galaxies with existing measurements of Virgo cluster galaxies and isolated field galaxies. We will compare these results to simulations of cluster growth and semi-analytic models of gas consumption to help identify the physical mechanisms that deplete galactic gas in dense environments, a key aspect required to understand galaxy evolution.

Most previous studies that look at the influence of environment on galaxy gas and star formation properties classify environment in terms of either cluster-centric radius or local density. However, the distribution of galaxies is not smooth, even near clusters. In this proposal, we move beyond to look as galaxies along two filaments that are feeding a group and cluster.

## 2. Scientific Motivation

A wealth of previous work has established that the fraction of quiescent (non star-forming) galaxies increases with stellar mass and environmental density (e.g. Dale et al. 2001; Kauffmann et al. 2004; Peng et al. 2010). However, the physical processes that deplete a galaxy's gas content and thus star formation remain unclear. In this proposal, we are focusing on where and how environment affects galaxies. While interactions with the intracluster medium clearly strip gas from some infalling cluster galaxies (e.g. Chung et al. 2007), there is ample evidence that galaxy SFRs are suppressed at distances up to  $\sim 5$  virial radii from cluster centers (Lewis et al. 2002; Bahé et al. 2013). This suggests that galaxies are being processed by dense environments before they fall into clusters (e.g. Poggianti et al. 1999; Cortese et al. 2006).

Despite clear evidence for intrinsic and environmental quenching of star formation, the physical processes underlying these correlations are not well known. Intrinsic processes may quench star formation through ejection or heating of the gas without impacting the distribution of existing stars (e.g. Springel et al. 2005; Croton et al. 2006; Dekel & Birnboim 2006). External or environmentally-driven processes such as tidal interactions and mergers can affect the distribution of both gas and stars (Springel et al. 2005; Croton et al. 2006; Dekel & Birnboim 2006), whereas pressure-driven interactions are expected to act primarily on the gas. For example, starvation, which results from a galaxy being cutoff from its supply of cold

gas (Larson et al. 1980), is expected to result in truncated gas disks while the spatial distribution of the remaining disk gas is circularly symmetric and the stellar disk is unaffected (e.g. Kawata & Mulchaey 2008). The interaction of galactic disk gas with the intracluster medium via ram-pressure stripping can remove the gas and produce asymmetries in the remaining disk gas (e.g. Quilis et al. 2000; Crowl et al. 2005). The environmental effects thus have different signatures on the relative abundances and spatial distribution of the warm ionized gas and molecular gas. By observing both phases, we can distinguish between these processes.

Large galaxy redshift surveys have revealed that galaxies are distributed in a complex network of matter with a large dynamic range of local density, called the cosmic web or filamentary structures (Kitaura et al. 2009; Darvish et al. 2014). These structures are seen in striking clarity around the Virgo cluster as shown in the top panel of Figure 1. Our goal is to understand how galaxies are altered as they move through the cosmic web and enter the densest regions. We are therefore in the midst of a multi-wavelength study of galaxies at a variety of positions in the cosmic web surrounding the Virgo cluster, one of the best studied regions of high density in the Universe.

background of filaments - galaxies fall into clusters along the filaments.

galaxies change colors in dense environments.

story - as large scale structure forms, galaxies in dense environments are different than field environment. growth of structure must affect galaxy properties. where is this happening.  
simulation picture - red and blue picture - what is relationship

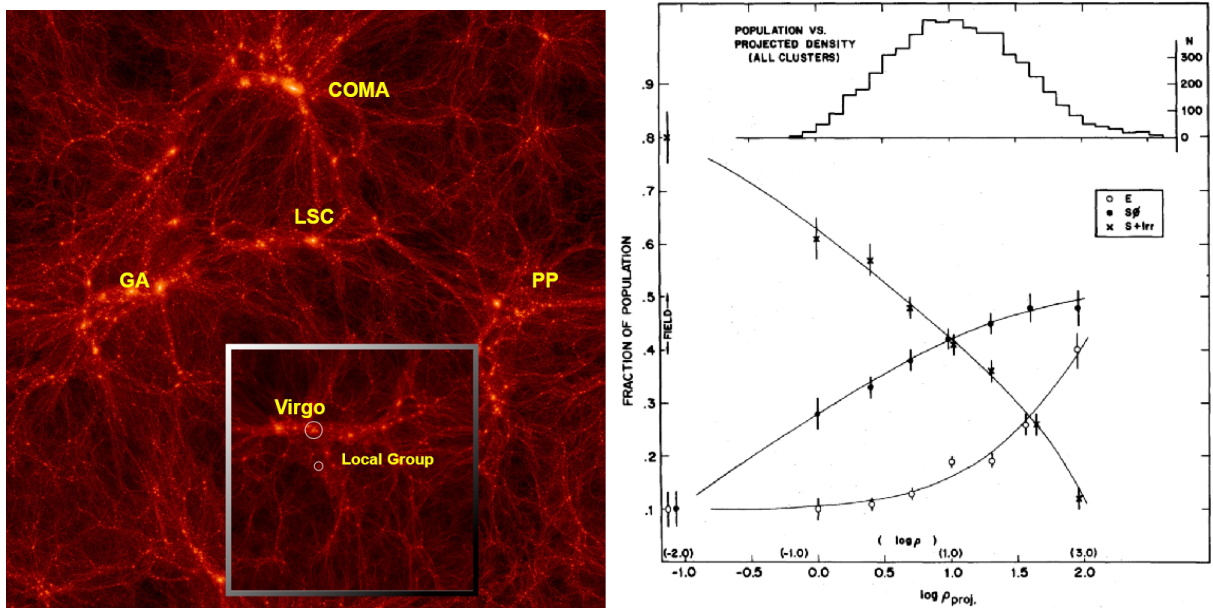


Fig. 1.— Simulation showing filaments feeding cluster. data showing how red fraction changes with environment.

Hydrodynamic simulations of cluster infall regions predict that the regions in filaments with the highest density gas can enhance the ram pressure in filaments by up to a factor of  $\sim 100$  (Bahé et al. 2013). This means that freshly infalling galaxies with  $\log(M_\star) < 9.5$  near a massive cluster can be stripped of their cold gas even well outside the virial radius. For more massive galaxies and at larger distances from the cluster, the ram pressure in filaments is still sufficient to strip off the hot gas that will replenish the dense star-forming gas, although it will likely not affect the densest cold gas. Filaments may therefore be the key sites where galaxies are affected by their environments before they fall into clusters.

### 3. Gas and Dust Content of Virgo Filament Galaxies

We propose to explore the physical properties of galaxies in the filaments around the Virgo cluster. Our approach differs from and complements previous works, as it moves away from the simple field/group/cluster trilogy. We follow instead the complex network of galaxies around a well studied cluster. Virgo is an ideal target as it is one of the best studied clusters. However, there is only sparse data on galaxies in the well-defined filaments leading into Virgo from large radii, making our project especially timely. The study of these filaments will benefit from the comparison with the rich ensemble of data already obtained for the center of Virgo: the atomic gas with the VLA by Chung et al (2009), and also at large scale with ALFALFA (Giovanelli et al. 2005); the dust content with the Herschel Virgo Cluster Survey (Davies et al. 2010); the stellar mass with the NGVS survey and WISE (Ferrarese et al. 2012); and recent star formation from UV data with GALEX GUViCS survey (Boselli et al. 2011).

#### 3.1. The Filament Galaxy Sample

Tully (1982) first studied the large-scale structure around the Virgo cluster and identified several concentrations of galaxies that he termed clouds. More recently Kim et al. (2016) repeat this analysis with a much larger spectroscopic dataset that probes to lower luminosities, and they are able to identify multiple filaments around Virgo, some that lead directly into the cluster and others that are nearby but not falling into Virgo. We show these filaments in Figure 4. This proposal focuses on two of the filaments identified by Kim et al. (2016), and we highlight these in the bottom panel of Figure 1. The NGC5353 filament feeds the NGC5353 group and extends over 20 Mpc, passing close to but not into the Virgo cluster (Kim et al. 2016). The second filament that we will study is the Leo filament. Kim et al. (2016) show that once you project galaxies into a Virgo-centric coordinate system (see right panel of Figure 4), galaxies in this region exist in three distinct filaments. We will target all of these. We focus on the NGC5353 and Leo filaments for two practical reasons: (1) these filaments extend the furthest north on the plane of the sky, and this allows for a longer observing window from northern hemisphere telescopes, (2) these filaments are among the most distant of the Virgo filaments and thus the galaxies have smaller apparent size. This helps to minimize the aperture correction that we need to apply to CO observations because when the galaxy size extends beyond the beam size.

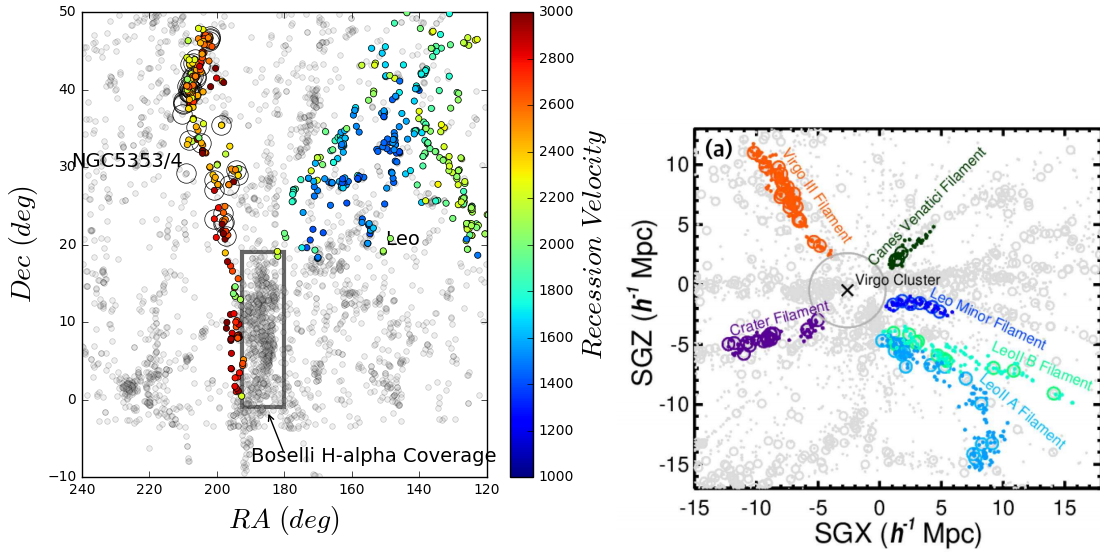


Fig. 2.— (Left) Figure 1(a) from Kim et al. (2016) showing filaments surrounding Virgo Cluster as observed on the plane of the sky in RA and Dec. (Right) Figure 2(a) from Kim et al. (2016) showing the same galaxies but projected into Virgo-centric coordinates. The Leo filaments can now be seen as three distinct filaments. The NGC5353 filament, which does not intersect the Virgo Cluster, is not shown in the right panel.

We show the  $NUV - r$  color versus stellar mass in Figure 3. The grey circles show all the filament galaxies that are in the NASA-Sloan Atlas. The green points show points that we will target with CO observations. We have restricted the mass range for the CO sample to  $9 < \log_{10}(M_\star/M_\odot) < 10$ . Galaxies below this mass limit are difficult to detect in CO due to lower metallicity and photodissociation of CO (ref). We set the upper limit to the mass range because we expect that galaxies with  $\log(M_\star/M_\odot) < 10$  will be most affected by the environment. We will push above this mass limit as telescope time permits.

The blue circles in Figure 3 show galaxies that we will target with  $H\alpha$  imaging. The  $H\alpha$  subsample includes all galaxies with  $8.5 < \log_{10}(M_\star/M_\odot) < 10$ . A total of 95 of these are in the NGC5353 filament and the remaining 126 are associated with the Leo filaments. The observations, data reduction, and analysis of the  $H\alpha$  imaging comprises the main thrust of this proposal.

The second main goal of this project is to map the spatial distribution of dust within the filament galaxies using WISE 12 $\mu$ m imaging. The open red circles in Figure 3 show 184 galaxies that are detected at 12 $\mu$ m by WISE with a signal-to-noise ratio above 10. We set this as the lower limit so that we have sufficient signal for fitting a two-dimensional Sérsic model, and we discuss the details of our image fitting in Section 3.2.3.

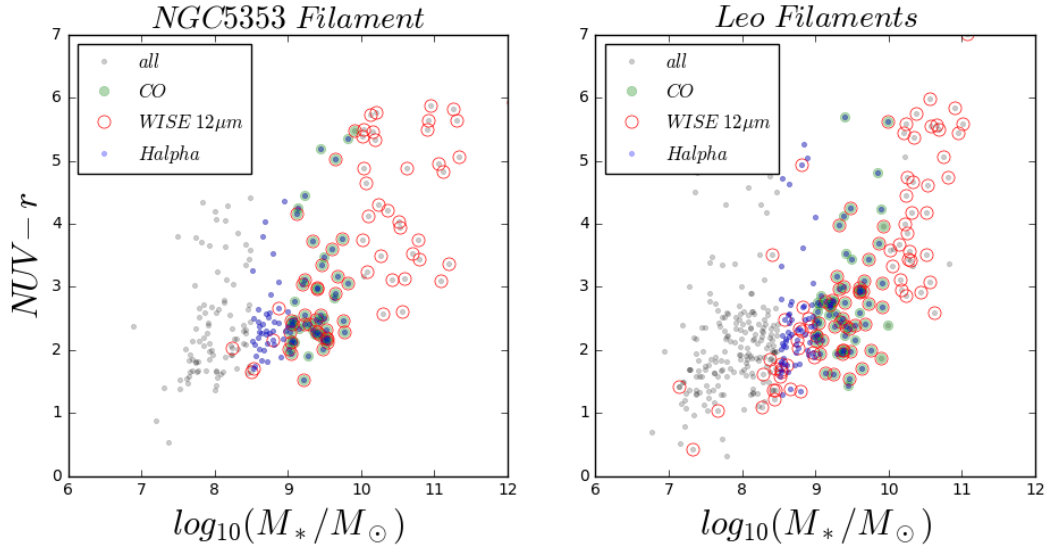


Fig. 3.—  $NUV - r$  color versus stellar mass for galaxies in the (left) NGC5353 filament and the (right) Leo filaments. The grey circles show all the filament galaxies that are in the NASA-Sloan Atlas, and the red circles show all galaxies that are detected at  $12\mu\text{m}$  by WISE with a signal-to-noise ratio above 10.

### 3.2. Methodology

Several groups have shown the power of panchromatic galaxy surveys - SINGS, THINGS, LITTLE THINGS - for understanding the complicated interplay between warm and cold interstellar medium. We take a similar approach, providing a complete census of cold gas and dust, and look at how the filament environment affects the many components a galaxy's gas reservoir.

and here we propose  $H\alpha$  imaging to map the spatial distribution of the hot gas and derive integrated SFRs. The combination of  $H\alpha$  and CO observations will allow us to calculate gas consumption timescales, characterize multiple phases of the galactic gas, and look for signatures of environmentally-driven depletion.

#### 3.2.1. Molecular and Atomic Gas

existing CO observations for 80 galaxies in filament

XX of galaxies the three filaments have existing HI detects.

Some observations already planned to observe the remaining galaxies.

HI observations proposed; remaining from green bank

CO, IR, and Optical Observations: *We have approved CO(2-1) and (1-0) observations with*

the IRAM 30-meter telescope to characterize the molecular gas contents of 20 galaxies the Northeast filament. We will quantify the stellar and dust components using SDSS imaging, optical spectroscopy, and far infrared (WISE and/or IRAS) fluxes. Cutting off the hot gas supply or stripping the diffuse molecular gas is a likely precursor to the suppression of star formation as the galaxy will use up its cold gas on a timescale of  $\sim 2.3$  Gyr (Bigiel et al. 2011). Likewise, direct stripping of the cold gas will result in a suppression of the CO and infrared luminosity and truncated  $H\alpha$  emission (e.g. Koopmann et al. 2004). Therefore, we expect a variety of gas effects to be observable by observing a sample of galaxies in both  $H\alpha$  and CO. Note that Virgo is the closest relatively massive cluster. There is no counterpart in which the major question of the origin of star formation quenching could be addressed in such exquisite details.

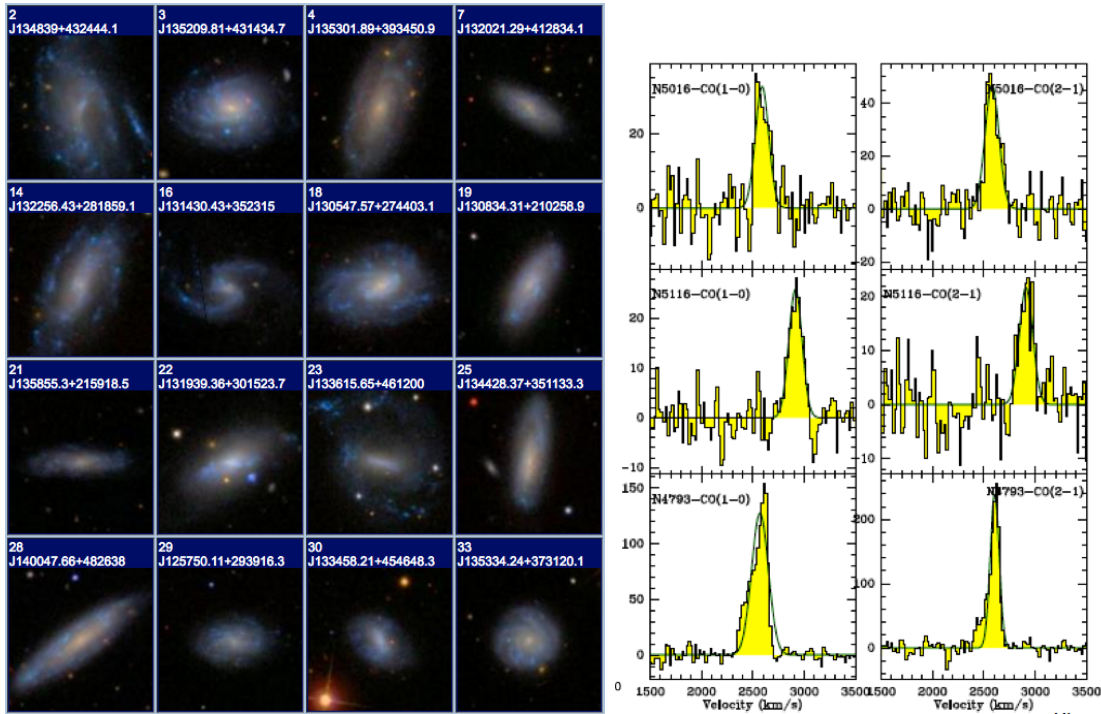


Fig. 4.— (Left) SDSS color images showing 16 randomly selected galaxies in NGC5353 filament. (Right) CO spectra from IRAM 30-m telescope for galaxies in the NGC5353 filament.

### 3.2.2. Ionized Gas and Current Star Formation Rates

The goal of our program is to obtain spatially resolved  $H\alpha$  maps for 222 star-forming galaxies in the NGC5353 and Leo filaments. These maps will allow us to test specific quenching mechanisms that involve the removal or rapid consumption of gas from galaxies. Key to accomplishing these goals are that we are able to measure  $H\alpha$  profiles to low surface brightness and that we can probe galaxies at different positions along the filament out to large

distances from Virgo.

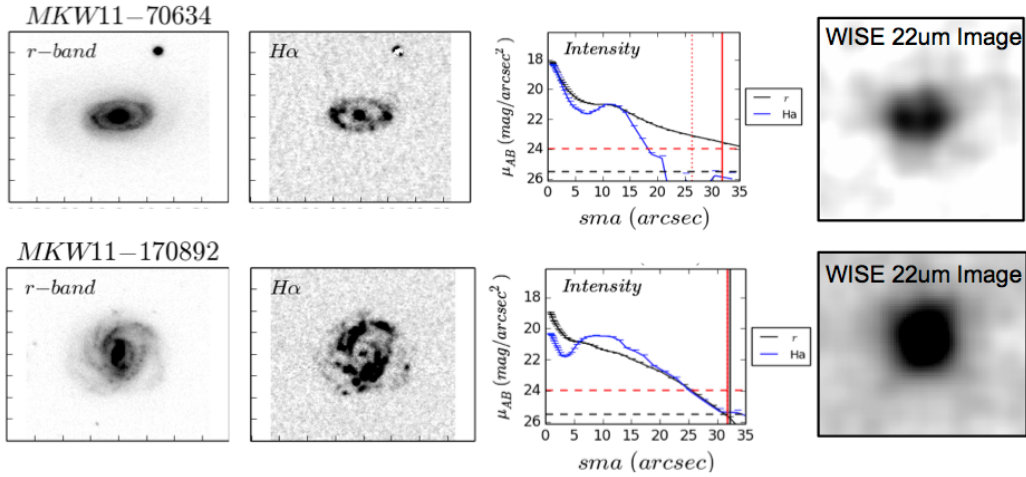


Fig. 5.— To illustrate our proposed  $H\alpha$  analysis, we show imaging taken with the KPNO 0.9-m+HDI of two galaxies within the nearby group MKW11 ( $v_r = 6900$  km/s). The left column shows a galaxy for which the star-forming disk probed by  $H\alpha$  is truncated along the semi-major axis (sma) relative to the stellar disk as probed in the  $r$ -band. The right column shows an example that is not truncated. The SFR is resolved at about 1/10 of a kpc in  $H\alpha$ . In contrast, the WISE PSF is 12 arcsec, corresponding to about 1 kpc. The image thumbnails in each row are the same size, demonstrating that the WISE data are not sufficient to measure the extent and morphology of the star formation. Indeed, the WISE photometry may underestimate the SFR for the lowest mass galaxies in our sample because of their low metallicity. As these galaxies are likely the most susceptible to stripping,  $H\alpha$  imaging is necessary to understand how environment affects their gas.

We will complete the  $H\alpha$  observations at the WIYN 0.9 and the Mt Laguna Observatory - Kansas has guaranteed time on the 1.2 m. For the WIYN 0.9 m, we will apply for time through NOAO, requesting approximately 6 nights each spring for the three years covered by this proposal. Based on past  $H\alpha$  imaging experience with the WIYN 0.9 m, we need about 2 hours per target, and so we expect to be able to complete 4 objects per night and 24 pointings per run. Our yield will be slightly higher ( $\sim 30$ ) because we will be able to place multiple objects within the  $0.5^\circ \times 0.5^\circ$  field of view. Thus we expect to complete  $H\alpha$  imaging for  $\sim 100$  galaxies at the WIYN 0.9m.

We will observe the remaining 120 galaxies in the  $H\alpha$  sample using the XX telescope at the Mount Laguna observatory. \*\*\* Background from Greg - commissioning, camera, FOV\*\* We have included funds to purchase an identical  $H\alpha + 4$  nm filter for this telescope.

To properly probe any environmentally-driven quenching, we must detect galaxies with star-formation rates below the star-forming main sequence. Elbaz et al. (2011) find that a  $\log_{10}(M_*/M_\odot) = 9$  galaxy has a SFR of  $0.25 M_\odot/\text{yr}$  at  $z = 0$ . The detection limits of our  $H\alpha$  imaging will allow us to detect galaxies with star-formation rates a factor of ten below

the star-forming main sequence.

We will measure the radial extent of the  $H\alpha$  emission and compare that to the extent of the stellar disks. Observations of the nearest galaxy clusters provide ample evidence that environment actively alters the gas content of infalling galaxies. Studies of the Virgo cluster show evidence of cold gas stripping (e.g. Koopmann & Kenney 1998, 2004; Dale et al. 2001; Crowl et al. 2005; Chung et al. 2007; Corbelli et al. 2012), including truncated  $H\alpha$  emission of Virgo spirals compared with their field counterparts (Koopmann & Kenney 2004). We will also measure integrated SFRs and use these to compute gas consumption times.

### 3.2.3. Dust Masses and Spatially-resolved Dust Maps

Infrared images are required to measure the spatial extent of dust-obscured star formation (and therefore the cold gas). WISE has observed the entire sky from 3.6-22 micron, providing the data required to make size measurements for a statistically significant galaxy sample spanning a large range of environments. While the WISE PSF is rather large ( $6.5''$  at  $12\mu\text{m}$ ), it still probes down to  $2 - 5$  kpc for galaxies in the redshift range we are focusing on, and is sufficient for this study. In contrast, Spitzer and Herschel data can be much more sensitive. However, they did not observe these filaments. Nevertheless, Spitzer and Herschel data will be used to validate the results based on the lower-sensitivity WISE data. In addition to providing a measure of the spatial extent of star formation, the WISE colors can be used to indicate the presence of an AGN. Along with the SDSS fiber spectroscopy, the WISE colors will be used to eliminate galaxies with infrared size measurements that are likely to be affected by an AGN.

we provide a qualitative example. In Figure 6, we show a spiral galaxy with  $12\mu\text{m}$  emission that is comparable in extent to the stellar disk. Again, comparing the  $r$  and  $24\mu\text{m}$  images shows a more extended star-forming disk, and the best-fit Sérsic models indicate that the  $24\mu\text{m}$  emission has an effective radius that is 90% of the stellar radius. Importantly, the  $12\mu\text{m}$  emission is again comparable in extent to the  $24\mu\text{m}$  emission.

The above examples show qualitatively that the  $12$  and  $24\mu\text{m}$  emission have a similar spatial extent. To provide a quantitative example, we show a preliminary GALFIT analysis for the  $12\mu\text{m}$  image of one spiral galaxy in Figure 7. The top panel shows the results for the  $12\mu\text{m}$  image, and the bottom set of images shows the best-fit for the  $24\mu\text{m}$  image. The best-fit models, shown in the center panels, have effective radii that agree within the errors. Thus, we conclude that the  $12\mu\text{m}$  images provide a suitable means of tracing the extent of the star-forming disk.

The image fitting is already available for the  $r$ -band images from the NASA-Sloan Atlas (Blanton et al. 2011). Thus the main thrust of this proposal is to run GALFIT on the  $12\mu\text{m}$  images to measure the spatial extent of the star-forming disk. We are not able to use the  $22\mu\text{m}$  data for this purpose due to its lower resolution and sensitivity. To quantify the extent of the  $12\mu\text{m}$  emission, we will use *GALFIT* software (Peng et al. 2002) to fit two-dimensional

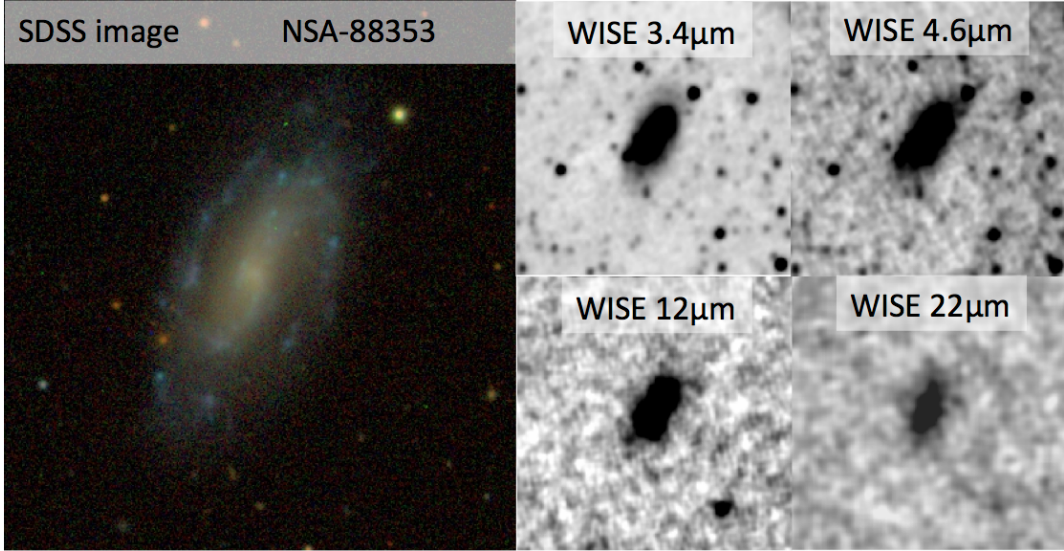


Fig. 6.— Multi-wavelength images of spiral galaxy NSA-88353. The 4 panels on the right are the WISE images. This galaxy has  $24\mu\text{m}$  emission that is comparable in extent to the stellar disk ( $r$ -band). The  $12\mu\text{m}$  emission is comparable in extent to stellar emission seen in SDSS and  $3.4\mu\text{m}$ .

*Sérsic* models to the galaxy images. We will use *unWISE* image products and PSFs (Lang 2014). We will use the best-fit parameters from the  $r$ -band as the initial guess for the  $12\mu\text{m}$  fits, holding PA and axis ratio fixed at the optical values. To test the sensitivity of our results to these initial conditions, we will stochastically vary the intial conditions to provide more robust estimates of range of acceptable fit parameters. This process is described in more detail below.

We will use simulated galaxies to test the reliability of our GALFIT model parameters. The WISE  $12\mu\text{m}$  data have lower resolution and lower signal-to-noise ratios than the optical imaging that GALFIT is typically used with. To test the reliability of the GALFIT models, we will create 1000 model galaxies and run them through our analysis. The model galaxies consist of single-component *Sérsic* models with randomly-selected parameters. The model galaxy will be created by first selecting a region on a WISE  $12\mu\text{m}$  tile that doesn't have a nearby object within 15 pixels. We will create a cutout of this region, generate a model galaxy using GALFIT, and then add the model and noise to the WISE cutout. We will then run the model through our analysis pipeline and compare the input and recovered parameters. This will help us determine the surface brightness limit of our survey.

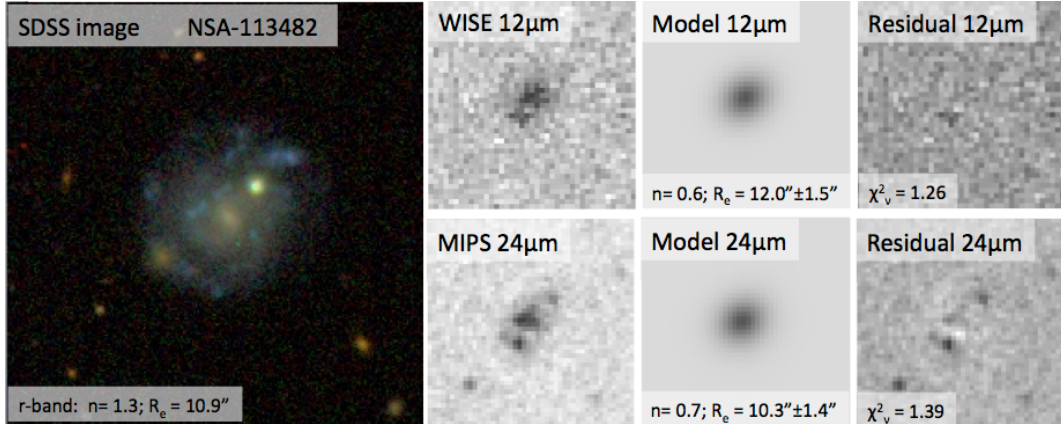


Fig. 7.— Color SDSS image of spiral galaxy NSA-113482 (left). The top row of three images shows the preliminary GALFIT analysis for the  $12\mu\text{m}$  image (top row). The three images show the  $12\mu\text{m}$  image (left), the GALFIT model (center), and the residual after the model is subtracted from the image. The bottom panels show the same for the MIPS  $24\mu\text{m}$  image. The model panels list the Sérsic profile and effective radius of the best-fit model, and the effective radii from the  $12$  and  $24\mu\text{m}$  fits agree within errors. This shows that  $12\mu\text{m}$  is a suitable means of tracing the extent of the star-forming disk.

### 3.3. Comparison with Theory

Constrained Local UniversE Simulations (CLUES) of local volume<sup>1</sup> includes dark matter, gas and stars.

The first scenario we must consider is whether our results are consistent with predictions of gas depletion through starvation and the consumption of the remaining gas rather than more extreme environmental processes such as ram-pressure stripping. In the left panel of Figure 8, we show the predicted size of the stellar and star-forming components of  $z = 0$  galaxies based on the semi-analytic models of Xie et al. (2016, in prep). These models include starvation but do not explicitly include environmental processes such as ram-pressure stripping. In the right panel of Figure 8, we show the *measured* size of the star-forming and stellar disks versus stellar mass for the *Local Cluster Survey* galaxies. While the size of the stellar disks are consistent with the model predictions, the size of the star-forming regions fall systematically below the model predictions. This indicates that additional environmental processes must be included to explain the small observed size of the star-forming region in these galaxies. However, the *Local Cluster Survey* sample is small and contains very few isolated/field galaxies. We need (1) a larger sample of cluster galaxies to confirm the inconsistency between model and observations, (2) a larger field sample to serve as a controlled comparison with the models, and (3) a more robust determination of the size of the star-forming region that includes a

<sup>1</sup><https://www.clues-project.org>

formal analysis of uncertainty.

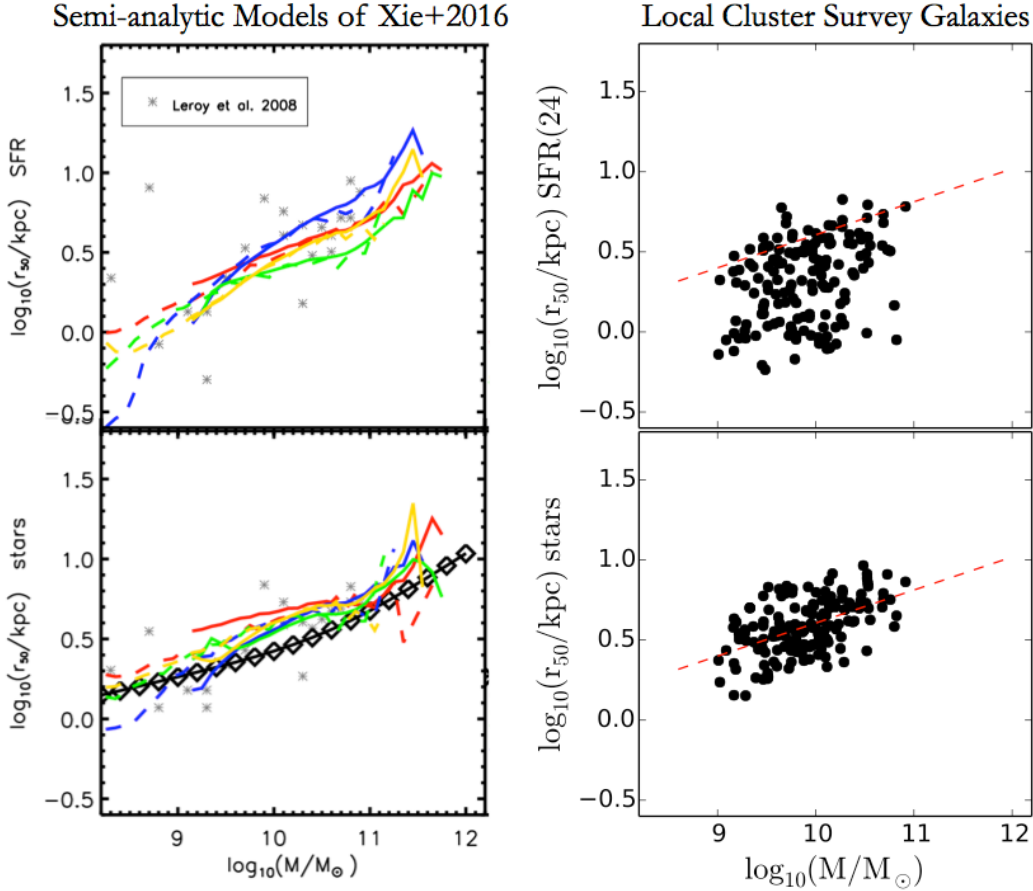


Fig. 8.— (left) **Predicted** half-light radius of stars (bottom) and star formation (top) versus stellar mass for  $z = 0$  galaxies (Xie et al. 2016, in prep). The different color lines represent different models for partitioning atomic and molecular hydrogen, and the grey points show comparison with some existing observations. (right) **Measured** half-light radius of stars (bottom) and star formation (top) versus stellar mass for galaxies in the *Local Cluster Sample*. The red dashed line is a linear fit to the stellar half-light radius and is shown in the top panel for comparison. The size of the star forming region is smaller than predicted by semi-analytic models, suggesting that starvation is not sufficient to explain the observed size of the SF region in these galaxies. A larger sample of galaxies with more robust size measurements is needed to confirm this result.

Theoretical models of ram-pressure stripping provide predictions that we can compare directly to our measurements. For example, numerical simulations of starvation and ram-pressure stripping of cold gas generically predict that star formation in the edges of galaxies will be affected more strongly than star formation near the centers of galaxies; the spatial extent of the star-forming disk should be smaller for galaxies that are undergoing stripping

(e.g. Kawata & Mulchaey 2008; Bekki 2014). We find evidence of this in the *Local Cluster Survey*, but we also find a stronger correlation with bulge-to-total ratio. A larger sample is needed to disentangle these effects. In addition, low mass galaxies should be more vulnerable to having their gas removed because the gas in lower mass galaxies is not as tightly bound (e.g. Kawata & Mulchaey 2008; McCarthy et al. 2007; Bekki 2014). We find some evidence of this in the *Local Cluster Survey*, but a larger sample is needed to strengthen the statistical significance.

### 3.3.1. Computational Requirements and Facilities:

Siena College has recently acquired a High Performance Computer Cluster. The cluster consists of 16 nodes each with two Intel Xeon E5-2630 6-core processors and 32 GB of RAM. The cluster has a total global storage capacity of 20.5 TB and 208 cores each running at 2.3 GHz. The Intel compiler suite is available to create efficient custom programs.

We estimate the computational complexity for analyzing 7000 galaxies with GALFIT in a systematic fashion. We would scan over the five-dimensional parameter space  $p=(x,y, \text{radius}, \text{concentration}, \text{brightness})$ , by discretizing each dimension from a minimum search value to a maximum one, and sweeping over the entire mesh of points. Assuming an average of 10 points per search direction, we have a lattice with  $10^5$  points. Preliminary analyses showed that the average fitting time is about 20 seconds with GALFIT. Therefore, the total computational time for scanning the entire parameter space is of the order  $1.4 \times 10^{10}$  seconds, which is prohibitively high for the computational resources at Siena College. However, there is no need to sample over ALL the points, since we are interested only in the number of the basins of attraction of each value  $p_*$ . In other words, GALFIT provides a direct way to map all possible starting points  $\{p\}$  to a subset of points  $\{p_*\}$  of 'best fit' points. Since the minimization algorithm used by GALFIT is the Levenberg-Marquardt algorithm, or downhill gradient, one can safely assume that around the minimum  $p_*$ , the best fit function is quadratic. We can therefore estimate the Hessian numerically around such point and extrapolate the size of the basin of attraction. In this way we can remove a number of points  $\{p\}$  from subsequent sweeps, as they would likely converge to the same attractor  $p_*$ . We cannot estimate the size of the basins of attraction precisely, nor the number of minima  $p_*$ , at this stage. For instance, if we find that only one or two minima exist, then quickly 50% to up almost 100% of the points can be skipped in the subsequent sweeps, because they would not bring any additional information. The calculation would be quite fast in this case. A higher number of local minima will only be detected by systematically sampling phase space.

We are also considering a stochastic sampling of the parameter space, by alternating a Monte Carlo sampling with the gradient minimization algorithm (Pardo et al. 2011). The code would be serial, but optimized for speed. In this case, the statistical errors decrease with  $1/\sqrt{N}$  where  $N$  is the number of sampling points in the parameter space. If  $N=1000$

the relative error is of the order of 3%, which is acceptable. Such an error is independent from the number of dimensions of the parameter space. Therefore stochastic sampling will have a definitive advantage. By running it on the HPCC of Siena College, it would take about 8 days of computational time. The test and exploratory runs are anticipated to take an additional 50 CPU hours (for a recent application of this method see, Sala et al. 2012).

The two computational techniques described above are sufficient to create a map of the full phase diagram accurately. In addition, we will compare the GALFIT results to those generated by other independent fitting programs such as GALPHAT (Yoon et al. 2011) and The Tractor (Lang et al. 2016).

### 3.4. Workplan, Major Milestones, and Timeline for Completion

Rose Finn, Ph.D., is a professor in the Department of Physics and Astronomy at Siena College (Loudonville, NY). She is the PI of the *Local Cluster Survey* and has extensive experience with running GALFIT on MIPS 24 $\mu$ m imaging. She will lead the analysis of the WISE 12 $\mu$ m imaging, lead the  $H\alpha$  imaging survey at KPNO, supervise the undergraduate students, and draft the paper.

Vandana Desai, Ph.D., is an astronomer at the NASA/IPAC Infrared Science Archive (IRSA). Vandana has extensive experience in all aspects of infrared astronomy and will lead technical aspects associated with the WISE data. She also is well-versed in best-practices of data sharing and will lead our efforts to disseminate data products over the web.

Graziano Vernizzi, Ph.D., is an associate professor at the Department of Physics and Astronomy of Siena College (Loudonville, NY). His research interests lie in computational and theoretical physics, biophysics, nanoscale science, soft condensed matter, and random matrix theory. Graziano will lead the computational aspects of this project.

Gregory Rudnick, Ph.D., is an associate professor at the University of Kansas. He has expertise in galaxy evolution, and he is leading an *HST* study to measure the spatial extent of star-formation in intermediate-redshift galaxies. He will lead the  $H\alpha$  imaging survey at XX observatory. Will supervise XX students.

Gabriella De Lucia, Ph.D, is a permanent research scientist at INAF - Astronomical Observatory of Trieste. Gabriella provides expertise in semi-analytic modeling of galaxy evolution. She is working on models that predict the spatial extent of the stellar and star-forming disks, and her work is thus extremely pertinent to this proposal. She will lead the theoretical interpretation of our results and the comparison with semi-analytic models of gas consumption.

Pascale Jablonka

Francoise Combes, PhD, is a Professor at College de France, and astrophysicist at Paris Observatory. She is an expert in the dynamics of galaxies, their star formation (SF) efficiency

and feedback processes, including the action of a super-massive black hole. She has made numerical simulations to test the processes of SF quenching, ram pressure stripping, tidal interaction, or strangulation. She will observe the cold gas content of galaxies in the Virgo filaments, the atomic (HI) or molecular (CO) reservoirs.

A total of 12 Siena College undergraduates students will be involved in this project over the course of three summers. During the first summer, the students will work on cross-matching our galaxy sample with ALFALFA, GIM2D structural fits, and the unWISE photometric catalogs. During the second summer, the students will analyze the star-forming main sequence using the WISE-derived star-formation rates.

The major milestones and timeline for completion are listed in Table 1.

### 3.5. Data Sharing and Further Dissemination of Results

We will produce a variety of measurements of the gas content of filament galaxies. We will produce a catalog of CO, HI, dust, Halpha properties to be released with our final paper.

While this data set of derived information will not be exceptionally large in volume, it will be of value to other observational astronomers and theorists working on galaxy evolution. To facilitate the widespread use of these data, we will publish the full catalog of measured and derived quantities on the web and in the on-line version of Astrophysical Journal Supplement. In addition, we will work with the NASA/IPAC Extragalactic Database (NED) to ensure that our data are discoverable to a larger user base. Co-I Vandana Desai, resident at IPAC, will act as our NED liaison to ensure that this gets done in a timely manner.

## 4. Broader Impact

### 4.1. Modeling Physics for High School Programs

The modeling approach is an innovative and effective way to teach physics that is fundamentally different from traditional techniques. Students are led through carefully constructed experiments and exercises to clearly develop the conceptual, visual, and mathematical models of how physics works. Experienced physicists already have these mental models, but beginning physics students do not. These models are essential for understanding physics. The modeling approach minimizes lectures, and instead students are actively engaged in collecting and analyzing real-time data that illustrate the fundamental concepts of physics. The students must then construct models to interpret these data.

As a former high school teacher, I know first-hand the importance of bringing the more effective and engaging techniques to the front line. As part of a previous NSF grant (AST-08XX), we have offered modeling workshop for high school physics teachers for the past 9 summers. We are fortunate to have as an adjunct instructor an area high-school physics teacher who is an expert in using the modeling approach to teach physics, and he will continue to lead these workshops. We offer 6 hours of continuing education credit to participants that can be used toward teacher recertification. This grant will provide a stipend for Darren

Broder to organize and lead the workshops. In successive years, Darren's compensation will be supported by registration fees from participating teachers. To assess the impact of the modeling curriculum, participating teachers will administer the force concept inventory and mechanics baseline test. In collaboration with Darren Broder, I will develop another assessment test for Electricity and Magnetism.

Each spring, the School of Science will help sponsor a dinner for area math and science teachers. The goal of this is two-fold. First, we will have a Siena student present on a recent research project so that the teachers become better acquainted with the opportunities for Siena students. Second, the teachers will have time for informal conversations to exchange teaching ideas and materials.

#### **4.2. Undergraduate Summer Research**

The importance of undergraduate research is widely recognized in the science community. *Recent studies have shown that undergraduate research may be the pedagogy for the 21<sup>st</sup> century (e.g., Council on Undergraduate Research Statement and references therein).* Involvement in research projects fosters highly motivated, self-confident students with enhanced analytical and communication skills.

Four Siena students began the first stages of their research projects this summer, and I expect all of these students to continue their involvement through the next academic year. Graduating students will be replaced by interested freshman or sophomores to maintain a total of 4 undergraduate researchers at any one time. Specific goals for current and future student researchers are:

- learn how to use python for image reduction and analysis
- identify correlations between optical and Hydrogen properties of galaxies and look for variations in these correlations as a function of galaxy environment

An important part of the research experience is presenting results to the community. I will encourage all students to present their results at the fall meeting of the Astronomical Society of New York and Siena's Academic Celebration, which is held each spring. In addition, I will strongly encourage seniors to present a poster at the annual winter meeting of the American Astronomical Society.

To assess the impact of this project, I will track participation, papers, presentation, and post-graduate activity of all Siena students who are involved in this project. I will design and implement a survey to assess student plans/goals before, during, and after participation in research.

#### **5. Summary**

##### **Intellectual Merit:**

**Broader Impact:** This proposal resonates with the National Science Foundation's broader impacts criteria on many levels. First, the proposal helps promotes teaching and learning by promoting modeling approach to teaching HS physics, integrating problem-based learning into general physics, and the introduction an astronomy concentrations within the physics major to increase the number of majors. Nationally, astronomy traditionally draws a higher fraction of women than physics, so the introduction of the astronomy concentration should attract more female students, a group that is significantly under-represented in phyiscs. Second, the project provides hands-on training and learning for tens of undergraduate students through research. The Siena undergraduate students will be encouraged to become involved in all aspects of research, including data aquisition at world-class observatories, on-campus data reduction and analysis, and presentation of results at national conferences and through publication in peer-reviewed journals. The computer analysis, data interpretation, and presentation skills the undergraduates learn will be essential for success in the workplace, the classroom, or graduate education in any field of science. Finally, the proposal enhances the infrastructure for research and education at Siena College by formalizing collaborations with the ALFALFA team, several of whom are located in New York State and already serve as an extended network of mentors for Siena undergraduates. The proposal will also enable Siena to conduct remote observing sessions at Arecibo.

**Broad Dissemination of Results:** The scientific results of will be disseminated broadly through publication in peer-reviewed journals, online database, presentation at regional, national and international meetings. I will provide a full catalog for the scientific community that will include an extensive array of primary and derived data products. This will be a much-needed reference for galaxy evolution modelers, particularly those who model the evolution of galaxies. The pedagogic results will also be disseminated broadly through publication in peer-reviewed journals and presentations at regional and national conferences. Of particular interest is the impact that problem-based learning has on student retention and research readiness. In addition, we will develop a new assessment tool that measures a student's ability to think independently and solve real-world problems. This will be of wide interest to institutions looking to implement similar research-focused curricular changes.

Table 1: Major Milestones and Schedule

Timeline		Responsibilities			Dissemination
		Finn	Desai	Vernizzi	
<b>Year 1 (2017)</b>	Spring	Finalize sample selection; identify and remove AGN; write code to retrieve cutouts from <i>unWISE</i> ; calculate stellar masses	Identify best techniques for modeling WISE PSF	Adapt GALFIT code to run on Siena computer cluster; develop code to run image analysis on parallel computing system	
	Summer	Supervise summer students - cross match sample with other surveys (AL-FALFA, GIM2D, <i>unWISE</i> photometry); identify groups and clusters within survey region; calculate environment parameters such as local density	Fit IR templates to estimate IR luminosity and SFRs for galaxies	Run code on computer cluster for a subset of the sample; adjust code and methodology as needed	
	Fall	Cross-check results with size measurements from MIPS data; run simulations to understand reliability limits	Interface with NED to plan for web release	Run code on complete sample	
<b>Year 2 (2018)</b>	Spring	Continue with analysis of full sample.			Poster at Jan 2018 AAS on preliminary results
	Summer	Finalize analysis; supervise summer students (star-forming main sequence as a function of environment); draft paper	Help draft paper; supervise web dissemination	Help supervise summer students; help draft paper	Make data products publically available through NED
	Fall	Continue with analysis of full sample.			present results at topical meeting; publish paper; release data to web

## REFERENCES

- Bahé, Y. M., McCarthy, I. G., Balogh, M. L., & Font, A. S. 2013, MNRAS, 430, 3017
- Bekki, K. 2014, MNRAS, 438, 444
- Blanton, M. R., Kazin, E., Muna, D., Weaver, B. A., & Price-Whelan, A. 2011, AJ, 142, 31
- Boselli, A., Boissier, S., Heinis, S., Cortese, L., Ilbert, O., Hughes, T., Cucciati, O., Davies, J., Ferrarese, L., Giovanelli, R., Haynes, M. P., Baes, M., Balkowski, C., Brosch, N., Chapman, S. C., Charmandaris, V., Clemens, M. S., Dariush, A., De Looze, I., di Serego Alighieri, S., Duc, P.-A., Durrell, P. R., Emsellem, E., Erben, T., Fritz, J., Garcia-Appadoo, D. A., Gavazzi, G., Grossi, M., Jordán, A., Hess, K. M., Huertas-Company, M., Hunt, L. K., Kent, B. R., Lambas, D. G., Lançon, A., MacArthur, L. A., Madden, S. C., Magrini, L., Mei, S., Momjian, E., Olowin, R. P., Papastergis, E., Smith, M. W. L., Solanes, J. M., Spector, O., Spekkens, K., Taylor, J. E., Valotto, C., van Driel, W., Verstappen, J., Vlahakis, C., Vollmer, B., & Xilouris, E. M. 2011, A&A, 528, A107
- Calzetti, D., Kennicutt, R. C., Engelbracht, C. W., Leitherer, C., Draine, B. T., Kewley, L., Moustakas, J., Sosey, M., Dale, D. A., Gordon, K. D., Helou, G. X., Hollenbach, D. J., Armus, L., Bendo, G., Bot, C., Buckalew, B., Jarrett, T., Li, A., Meyer, M., Murphy, E. J., Prescott, M., Regan, M. W., Rieke, G. H., Roussel, H., Sheth, K., Smith, J. D. T., Thornley, M. D., & Walter, F. 2007, ApJ, 666, 870
- Chung, A., van Gorkom, J. H., Kenney, J. D. P., & Vollmer, B. 2007, ApJ, 659, L115
- Corbelli, E., Bianchi, S., Cortese, L., Giovanardi, C., Magrini, L., Pappalardo, C., Boselli, A., Bendo, G. J., Davies, J., Grossi, M., Madden, S. C., Smith, M. W. L., Vlahakis, C., Auld, R., Baes, M., De Looze, I., Fritz, J., Pohlen, M., & Verstappen, J. 2012, A&A, 542, A32
- Cortese, L., Gavazzi, G., Boselli, A., Franzetti, P., Kennicutt, R. C., O’Neil, K., & Sakai, S. 2006, A&A, 453, 847
- Croton, D. J., Springel, V., White, S. D. M., De Lucia, G., Frenk, C. S., Gao, L., Jenkins, A., Kauffmann, G., Navarro, J. F., & Yoshida, N. 2006, MNRAS, 365, 11
- Crowl, H. H., Kenney, J. D. P., van Gorkom, J. H., & Vollmer, B. 2005, AJ, 130, 65
- Dale, D. A., Giovanelli, R., Haynes, M. P., Hardy, E., & Campusano, L. E. 2001, AJ, 121, 1886
- Darvish, B., Sobral, D., Mobasher, B., Scoville, N. Z., Best, P., Sales, L. V., & Smail, I. 2014, ApJ, 796, 51

- Davies, J. I., Baes, M., Bendo, G. J., Bianchi, S., Bomans, D. J., Boselli, A., Clemens, M., Corbelli, E., Cortese, L., Dariush, A., De Looze, I., di Serego Alighieri, S., Fadda, D., Fritz, J., Garcia-Appadoo, D. A., Gavazzi, G., Giovanardi, C., Grossi, M., Hughes, T. M., Hunt, L. K., Jones, A. P., Madden, S., Pierini, D., Pohlen, M., Sabatini, S., Smith, M. W. L., Verstappen, J., Vlahakis, C., Xilouris, E. M., & Zibetti, S. 2010, *A&A*, 518, L48
- Dekel, A. & Birnboim, Y. 2006, *MNRAS*, 368, 2
- Ferrarese, L., Côté, P., Cuillandre, J.-C., Gwyn, S. D. J., Peng, E. W., MacArthur, L. A., Duc, P.-A., Boselli, A., Mei, S., Erben, T., McConnachie, A. W., Durrell, P. R., Mihos, J. C., Jordán, A., Lançon, A., Puzia, T. H., Emsellem, E., Balogh, M. L., Blakeslee, J. P., van Waerbeke, L., Gavazzi, R., Vollmer, B., Kavelaars, J. J., Woods, D., Ball, N. M., Boissier, S., Courteau, S., Ferriere, E., Gavazzi, G., Hildebrandt, H., Hudelot, P., Huertas-Company, M., Liu, C., McLaughlin, D., Mellier, Y., Milkeraitis, M., Schade, D., Balkowski, C., Bournaud, F., Carlberg, R. G., Chapman, S. C., Hoekstra, H., Peng, C., Sawicki, M., Simard, L., Taylor, J. E., Tully, R. B., van Driel, W., Wilson, C. D., Burdullis, T., Mahoney, B., & Manset, N. 2012, *ApJS*, 200, 4
- Giovanelli, R., Haynes, M. P., Kent, B. R., Perillat, P., Saintonge, A., Brosch, N., Catinella, B., Hoffman, G. L., Stierwalt, S., Spekkens, K., Lerner, M. S., Masters, K. L., Momjian, E., Rosenberg, J. L., Springob, C. M., Boselli, A., Charmandaris, V., Darling, J. K., Davies, J., Garcia Lambas, D., Gavazzi, G., Giovanardi, C., Hardy, E., Hunt, L. K., Iovino, A., Karachentsev, I. D., Karachentseva, V. E., Koopmann, R. A., Marinoni, C., Minchin, R., Muller, E., Putman, M., Pantoja, C., Salzer, J. J., Scudegio, M., Skillman, E., Solanes, J. M., Valotto, C., van Driel, W., & van Zee, L. 2005, *AJ*, 130, 2598
- Kauffmann, G., White, S. D. M., Heckman, T. M., Ménard, B., Brinchmann, J., Charlot, S., Tremonti, C., & Brinkmann, J. 2004, *MNRAS*, 353, 713
- Kawata, D. & Mulchaey, J. S. 2008, *ApJ*, 672, L103
- Kim, S., Rey, S.-C., Bureau, M., Yoon, H., Chung, A., Jerjen, H., Lisker, T., Jeong, H., Sung, E.-C., Lee, Y., Lee, W., & Chung, J. 2016, ArXiv e-prints
- Kitaura, F. S., Jasche, J., Li, C., Enßlin, T. A., Metcalf, R. B., Wandelt, B. D., Lemson, G., & White, S. D. M. 2009, *MNRAS*, 400, 183
- Koopmann, R. A. & Kenney, J. D. P. 1998, *ApJ*, 497, L75
- . 2004, *ApJ*, 613, 866
- Lang, D. 2014, *AJ*, 147, 108

- Lang, D., Hogg, D. W., & Schlegel, D. J. 2016, AJ, 151, 36
- Larson, R. B., Tinsley, B. M., & Caldwell, C. N. 1980, ApJ, 237, 692
- Lewis, I., Balogh, M., De Propris, R., Couch, W., Bower, R., Offer, A., Bland-Hawthorn, J., Baldry, I. K., Baugh, C., Bridges, T., Cannon, R., Cole, S., Colless, M., Collins, C., Cross, N., Dalton, G., Driver, S. P., Efstathiou, G., Ellis, R. S., Frenk, C. S., Glazebrook, K., Hawkins, E., Jackson, C., Lahav, O., Lumsden, S., Maddox, S., Madgwick, D., Norberg, P., Peacock, J. A., Percival, W., Peterson, B. A., Sutherland, W., & Taylor, K. 2002, MNRAS, 334, 673
- McCarthy, I. G., Bower, R. G., Balogh, M. L., Voit, G. M., Pearce, F. R., Theuns, T., Babul, A., Lacey, C. G., & Frenk, C. S. 2007, MNRAS, 376, 497
- Pardo, L. C., Rovira-Esteva, M., Busch, S., Moulin, J.-F., & Tamarit, J. L. 2011, Phys. Rev. E, 84, 046711
- Peng, C. Y., Ho, L. C., Impey, C. D., & Rix, H.-W. 2002, AJ, 124, 266
- . 2010, AJ, 139, 2097
- Poggianti, B. M., Smail, I., Dressler, A., Couch, W. J., Barger, A. J., Butcher, H., Ellis, R. S., & Oemler, Jr., A. 1999, ApJ, 518, 576
- Quilis, V., Moore, B., & Bower, R. 2000, Science, 288, 1617
- Sala, G., Haberl, F., José, J., Parikh, A., Longland, R., Pardo, L. C., & Andersen, M. 2012, ApJ, 752, 158
- Springel, V., Di Matteo, T., & Hernquist, L. 2005, MNRAS, 361, 776
- Tully, R. B. 1982, ApJ, 257, 389
- Yoon, I., Weinberg, M. D., & Katz, N. 2011, MNRAS, 414, 1625